POTENTIAL OF SULFUROUS ACID,2-PROPYL UNDECYL ESTER (SPE) AND PENTAFLUOROPROPIONIC ACID, UNDECYL ESTER (PPE) AGAINST CORROSION OF MILD STEEL: COMPUTATIONAL APPROACH.

Saifullahi Lawal Muhammad, Muhammad Bashir Ibrahim, Muhammad Abubakar, Ayuba Abdullahi Muhammad, and Dahiru Adamu Gwarzo

Department of Chemistry, Federal University, Gashua, Yobe, Nigeria.

Department of Pure and Industrial Chemistry, Bayero University, Kano, Nigeria.

Department of Pure and Industrial Chemistry, Bayero University, Kano, Nigeria.

Department of Pure and Industrial Chemistry, Bayero University, Kano, Nigeria.

Department of Chemistry, Federal University, Gashua, Yobe, Nigeria.

ABSTRACT

Mild steel is the most commonly used metal in industries, however, mild steel corroded when exposed to certain amount of acid or base. Therefore, there is need to developed effective corrosion inhibitors to reduce the level of mild steel corrosion. This work evaluate the anticorrosion potential of two undecyl ester derivatives, namely: Sulfurous acid, 2-propyl undecyl ester (SPE) and Pentafluoropropionic acid, undecyl ester (PPE) against the corrosion of mild steel have been investigated using quantum chemical calculations and molecular dynamic simulation. Quantum chemical calculations were analyzed using several global parameters such as E_{HOMO}, E_{LUMO}, ΔE, μ, χ, I, A η, σ, ω, ε, $\Delta Eb\text{-}d$ and ΔN as well as local reactivity parameters which include condensed Fukui and second-order Fukui functions were used in describing and correlating the reactivity of the molecules with the computed descriptors. The adsorption behavior of the molecules on Fe (1 1 0) surface were analyzed using quenched molecular dynamic. The equilibrium adsorption configuration of the studied molecules shows that the molecules were adsorbed on Fe (1 1 0) surface in parallel orientation. The analyses of local reactivity indicated that the molecules have several points of nucleophilic and electrophilic attack. Hence, from the results of quantum chemical parameters and adsorption energy of the molecules on Fe (1 1 0) surface, the inhibition efficiency of the molecules follows the order of: SPE > PPE. The adsorption energy values of the two molecules are more negative than 100 kcal mol^{-1} indicating chemical adsorption between inhibitor molecules and metal surface.

Keywords: Zinc, corrosion, inhibitor, *azadirachta indica* (AI) leave extract, density functional theory (DFT), molecular dynamic simulation (MDS).

INTRODUCTION

Mild steel is regarded as the most commonly used ferrous alloy in industries due to its wide range of applications, excellent combination of mechanical properties, ease of fabrication, excellent weldability, and low purchasing cost. However, mild steel has a low corrosion resistance especially in acidic environment (Oke *et al*. 2018). Mild steel has extensively used under different conditions in chemical and allied industries in handling alkaline, acid and salt solutions. Chloride, sulphate, and nitrate ions in aqueous media are particularly aggressive and accelerate corrosion. Corrosion is the deterioration of metal by an attack from chemicals or reaction with their environment. It's a constant and continuous process, often difficult to abolish completely. Preventing the process from occurring will be more practical and achievable than complete abrogation (Srikanth and Sivakumar, 2020; Dubey, 2020).

Corrosion poses a serious problem in industries and society in general due continuous use of metals. The problem causes by corrosion on metals are destructive, resulting to mechanical failure and devaluation of products. It also causes degradation and eventually failure of components and systems in industries (Jane and Nakara, 2019). Aggressive medium are widely used in various industrial processes, such as oil well acidification, acid pickling, acid cleaning and acid descaling, which generally leads to serious metallic corrosion (Elmsellem *et al*. 2017). Therefore, it is necessary to control the corrosion of mild steel for its efficient utilization in various industrial processes. Among the methods of preventing corrosion of metals, the most cost-effective way is the use of corrosion inhibitors (Abakedi and Asuquo, 2016). The inhibitors can be organic or inorganic, and most credible option is the use of natural organic inhibitors as an eco-friendly. These are substances added in small concentrations to corrosive media to decrease or prevent the reaction of metals with the media (Ajanaku *et al*. 2015). These inhibitor molecules consist of heterocyclic compounds with popular functional groups (e.g. N, S, O, and P) and conjugated double bonds with different aromatic system. Basically, these substances are adsorbed on the metal surface thereby blocking the destruction reaction with aggressive media through physical or chemical adsorption mechanism (Sharma *et al*. 2015; Zarrouk *et al*. 2015).

The inhibition efficiency of the inhibitor molecules has been found to be strongly correlated with their molecular/electronic properties. The use of traditional methods, such as weight loss method, potentiodynamic polarization, and electrochemical impedance spectroscopy to perform this assignment is time consuming and too cost (Khaled and Muhammad, 2009; Umaru and Ayuba, 2020a). Therefore, theoretical approach which overcome such defect are highly recommended. Fortunately, with development of computer technology and the constant enhancement of the ability to deal with data, density functional theory (DFT) and molecular dynamic simulations (MDS) methods have becomes past and powerful tools to predict the corrosion inhibition efficiency of inhibitor molecules in recent times (Guo *et al*. 2020; Kaya *et al*. 2016).recent studies were carried out to model electronic, structural and molecular properties of compounds that have been established to be promising inhibitors are either in nature inorganic, organic or condensed matter (Ayuba *et al*. 2020; Ali-Shattle *et al*. 2021).

Quantum chemical calculations is theoretical tool that can be used to obtain molecular/electronic properties of the inhibitor molecules such as dipole moment, frontier molecular orbital energy, fraction of electron transferred from inhibitor molecule to metal surface, global hardness, softness and the rest (Sahin *et al*. 2008; Umaru and Ayuba, 2020b). In addition, chemical structure of the inhibitor molecules and its electronic properties plays a vital role in affecting the inhibition efficiency of the inhibitor molecules, making it difficult to correlate the electronic properties with inhibition efficiency (Madkour and Elshamy, 2016). In view of the above, this study focus on inhibitor molecules with similar structures that differ in position and type of heteroatom attached to the structures, this will facilitate the determination of the effect of electronic properties on the inhibition efficiency of the molecules. Molecular dynamic simulation has the capacity to provide the actual interaction and binding energy between the inhibitor molecule and metal surface (Ayuba *et al.* 2018a).

The aim of the present work is employ quantum chemical calculations and molecular dynamic simulation to evaluate the anticorrosion potential of undecyl ester derivatives, namely: Sulfurous acid, 2-propyl undecyl ester (SPE) and Pentafluoropropionic acid, undecyl ester (PPE) against the corrosion of mild steel without any wet chemical treatment. The extracts component utilized for computational analyses in this study were obtained from GC-MS analysis of neem tree leave extracts which are; Sulfurous acid, 2-propyl undecyl ester (SPE) and Pentafluoropropionic acid, undecyl ester (PPE), their structures are shown in Figure 1.
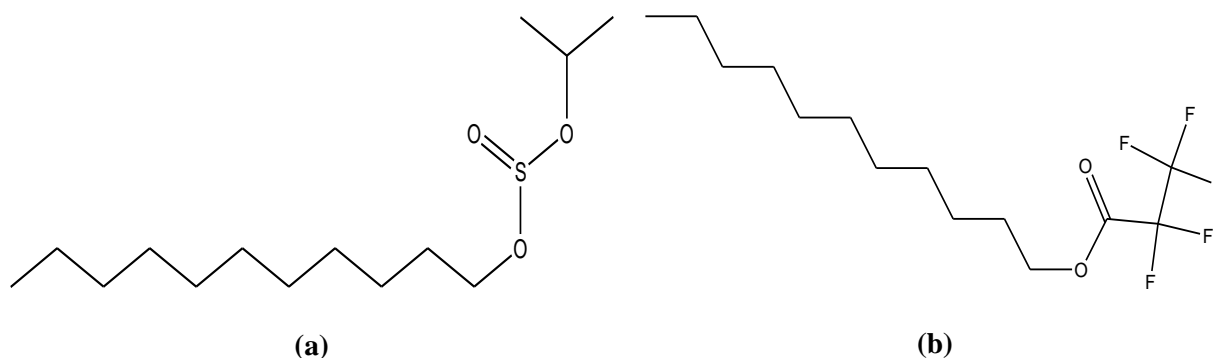
Figure 1: Chemical structures of the studied molecules: (a) Sulfurous acid, 2-propyl undecyl ester (SPE), (b) Pentafluoropropionic acid, undecyl ester (PPE)

RESEARCH METHOD

Quantum Chemical Parameters

The entire theoretical calculations were executed using the density functional theory (DFT) with function B3YLP and DND as the basic set programs in DMol^3 as contained in the material studio 8.0 software (Accelrys, Inc.) which provide an insights into chemical reactivity and selectivity, in terms of global parameters such as electronegativity (χ), hardness (η), and softness (σ), energy of the frontier molecular orbitals (E_{HOMO} and E_{LUMO}), frontier orbitals (HOMO and LUMO), energy gap (ΔE), and local ones such as the fukui function f(r) were evaluated using Koopman's theorem (Al-Mazaideh *et al*. 2016; Elmsellem *et al*. 2017; Khadom, 2017; Ayuba *et al*. 2020).

Global reactivity paraeters

Consequently, for an N-electron system with total total electronic energy E and an external potential v(r), the chemical potential μ, known as the negative of the electronegativity χ, has been defined as the first derivative of E with respect to N at constant v(r) as expressed in equation (1) (Umaru and Ayuba, 2020b).

$$\chi = -\mu = -\left(\frac{\partial E}{\partial N}\right) v(r) \qquad (1)$$

Hardness was defined within DFT as the second derivative of E with respect to N at constant v(r) as expressed in equation (2) (Umaru and Ayuba, 2020a).

$$\eta = \left(\frac{\partial E^2}{\partial N^2}\right) v(r) = \left(\frac{\partial u}{\partial N}\right) v(r) \qquad (2)$$

The ionization potential are defined as the negative energy of highest molecular orbital (E_{HOMO}), and electron affinity was defined as negative energy of lowest unoccupied molecular orbital (E_{LUMO}) which are expressed in equation (3) and (4) respectively (Elmsellem *et al*. 2017; Ayuba *et al*. 2020; Umaru and Ayuba, 2020b).

$$I = -E_{HOMO} \qquad (3)$$

$$A = -E_{LUMO} \qquad (4)$$

The absolute electronegativity (χ), and global hardness (η) of the inhibitor molecule are also related to this parameters mentioned above (Al-Mazaideh *et al*. 2016).

$$\chi = \frac{I+A}{2} \ , \ \chi = -\frac{1}{2}(E_{HOMO} + E_{LUMO}) \tag{5}$$

$$\eta = \frac{I-A}{2} \ , \eta = -\frac{1}{2}(E_{HOMO} - E_{LUMO}) \tag{6}$$

Global softness are defined in equation (7)

$$\sigma = \frac{1}{\eta} \tag{7}$$

The global electrophilicity index (ω) introduced by Parr (Madkour and Elshamy, 2016; El-Hendawy *et al*. 2021) is the inverse of nucleophilicty and is given in equation (9). The index is calculated using the electronic chemical potential and chemical hardness. In addition, nucleophilicity (ε) is the inverse of electrophilicity index as given in equation (8).

$$\varepsilon = {1}/{\omega} \tag{8}$$

$$\omega = \frac{\mu^2}{2\eta} = \frac{\chi^2}{2\eta} \tag{9}$$

Also, the energy change of the back donation of the molecule is directly proportional to the hardness of the molecule, as described in equation (10) (El-Hendawy *et al*. 2021).

$$\Delta E_{back-donation} = -\frac{\eta}{4} \tag{10}$$

The donation of an electrons from the inhibitor molecule to the Fe surface metal was calculated using the fraction of electron transferred (ΔN), in equation (11).

$$\Delta N = \frac{\chi_{Fe} - \chi_{Inh}}{2(\eta_{Fe} + \eta_{Inh})} \tag{11}$$

Where $\chi_{Fe} = 4.026 eV$, and χ_{Inh} stands for absolute electronegativity of mild steel and the inhibitor molecule respectively. $\eta_{Fe} = 3.875 eV$, and η_{Inh} stands for absolute global hardness of mild steel and the inhibitor molecule respectively (Benedetti *et al*. 2015; Al-Mazaideh *et al*. 2016).

Local reactivity

The local reactivity of the molecules were analysed through determination of Fukui indices. The Fukui indices are measures of chemical reactivity, as well as an indicative of the reactive regions and the nucleophilic and electrophilic behaviour of the molecule.

The Fukui function f(r) is defined as the first derivative of electron density q(r) with respect to the number of electrons N at constant external potential v(r). hence, using a scheme of finite difference approximations from mulliken population analysis of atoms in all the molecules under study and depending on the direction of electron transfer equation (12), (13), and (14) were used in the software for the calculations of nucleophilic attack f_K^+, electrophilic attack f_K^-, and radical attack f_K^0 respectively (Umaru and Ayuba, 2020b).

$$f_K^+ = q_k(N+1) - q_k(N) \qquad (12)$$

$$f_K^- = q_k(N) - q_k(N-1) \qquad (13)$$

$$f_K^0 = \frac{q_k(N+1) - q_k(N-1)}{2} \qquad (14)$$

Where q_k is the gross charge of atom k in the molecule that is the electron density at a point r in space around the molecule, N corresponds to the number of electrons in the molecule. N + 1 corresponds to an anion, with an electron added to the LUMO of the neutral molecule; N − 1 corresponds to the cation with an electron removed from HOMO of the neutral molecule. All calculations were done at the ground state geometry. These functions were condensed to the nuclei by using an atomic charge partitioning scheme, such as Mulliken population analysis in equation (12 − 14).

Second order fukui function (f^2) known as dual descriptor $\Delta f(k)$, is another local descriptor reported by (Umaru and Ayuba, 2020a), and it has been defined as the difference between nucleophilic and electrophilic fukui functions as expressed in equation (15).

$$f^2(r) = f_k^+ - f_k^- \qquad (15)$$

If $f^2(r) > 0$, then site k prefers nucleophilic attack, whereas if $f^2(r) < 0$, then site k prefers an electrophilic attack. Therefore, $f^2(r)$ serves as an index of selectivity towards nucleophilic or electrophilic attack.

Molecular Dynamic Simulation

Molecular Dynamic (MD) was carried out using forcite quench MD simulation house in the Material Studio 8.0 software (Accelrys, Inc.) so as to examine the interaction between the studied molecules and Fe surface. Hence, the optimized structure of the molecules and the Fe surface were utilized for simulation. This was aimed at sampling three different energy minima of the quenched dynamics in order to obtain an average global minimum (Umaru and Ayuba, 2020b; Ayuba *et al.* 2020). Among various Fe surfaces available, the cleaved Fe (1 1 0) plane was selected and utilized due to its stability and higher densely packed atoms.
The simulation were conducted on 6 x 5 Fe (1 1 0) surface using the smart algorithm and condensed-phase optimized molecular potentials for atomistic simulation studies (COMPASS) force field. To avoid possible molecular edging effects which may occur during the docking process, the built Fe slab was significantly relatively larger than the molecule to adequately accommodate the adsorbed molecule. The temperature for the simulation was maintained at 350K, 5ps simulation time and 1 fs time step.
The optimized Fe surface was utilized for docking process. The system quench was achieved every 250 steps with the Fe (1 1 0) atoms well constrained. To determine the energy of adsorption (E_{ads}) and the binding energies (BE) of the single molecule adsorbed onto the Fe (1 1 0) surface which provides access of relating them to inhibition efficiencies, the following equation (16) is used (Ayuba *et al.* 2020).
$$E_{ads} = -BE = E_{complex} - (E_{Zn} + E_{inhibitor}) \qquad (16)$$
Where $E_{complex}$ is the total energy of the Fe surface and inhibitor, E_{Fe} is the energy of the Fe surface without the inhibitor, and $E_{inhibitor}$ is the energy of the inhibitor without the Fe surface.

RESULT AND DISCUSSION

Frontier Molecular orbital

As explained earlier, the effectiveness of the inhibitor molecule does not only depend on molecular structure, but also on the electronic distribution of molecular orbitals. The HOMO region is associated with the electron donating ability of the molecule while LUMO region measures the electron accepting ability

of the molecules (Kaya *et al*. 2016). Figure (2-3) show the optimized molecules, electron density distributed around the studied molecules, HOMO and LUMO orbitals. It is apparent from the Figure 2 that both HOMO and LUMO are distributed mainly around the heteroatoms in the molecule, while Figure shows that the HOMO are distributed around the long chain and the LUMO center are distributed around the heteroatoms.

This indicate that area around the heteroatom in the SPE are the center for donation of electrons to the empty d-orbitals of the metal as well as accepting electrons from the metal through anti-bonding orbitals. In the case of PPE the long chain in the molecule serve as the center of donating electron while the area around the heteroatoms reflect the center for accepting electron from metal through back-donation.

Also from the geometry optimized molecules in (Figure 2 and 3), it was observed that all the molecules are almost planar in shape with PPE molecule tilted the mild steel surface which reduces the area of contact between the molecule and the metal surface, and as a result it has a low adsorption energy than SPE molecule which has planar shape and possess a parallel orientation that make it to have maximum area of contact with the mild steel surface.

Therefore, in this regard the trend in adsorption energy of the molecules follow: SPE > PPE. The electron density is saturated all around each molecule which ease parallel orientation of the molecules on the mild steel surface. Figure 2 and 3 indicate the electronic and structural properties of SPE and PPE.
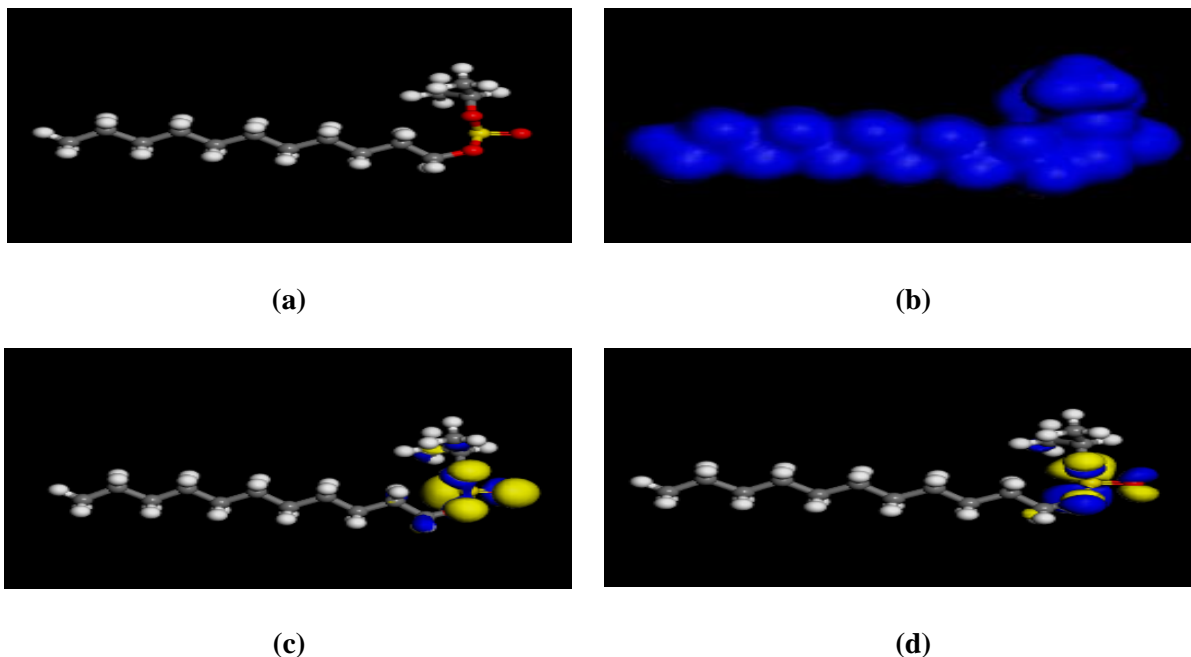

(a)

(b)

(c)

(d)

Figure 2: (a) Optimized Structure of SPE (b) Electron Density of SPE (c) HOMO Orbital for SPE (d) LUMO Orbital for SPE
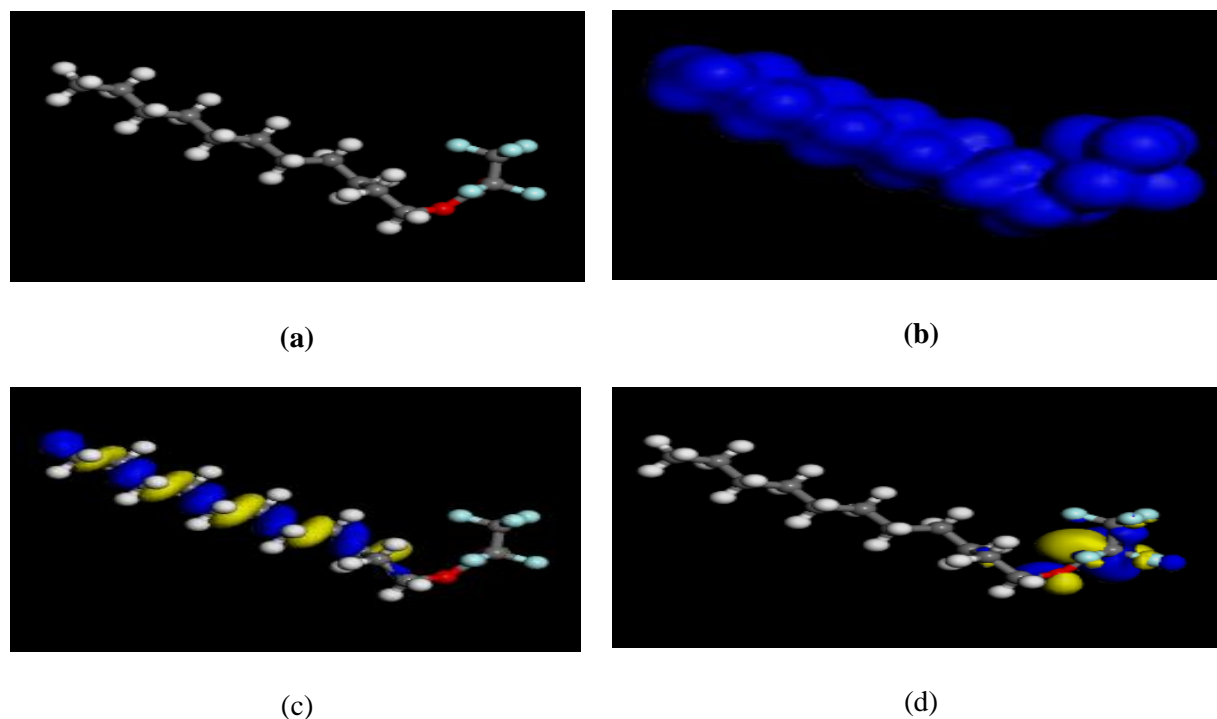
(a)

(b)

(c)

(d)

Figure 3: (a) Optimized Structure of PPE (b) Electron Density of PPE (c) HOMO Orbital for PPE (d) LUMO Orbital for PPE

Frontier Orbital Energies

The Frontier orbital energies of the two studied inhibitor molecules were compiled from quantum chemical calculations using Accryls Material Studio, 8.0 software (Ayuba *et al*. 2020) and presented in Table 1. Quantum chemical parameters evaluated include E_{HOMO}, E_{LUMO}, energy gap (ΔE), electronegativity, global softness, global hardness, the fraction of electron transferred from the inhibitor molecule to the metal surface (ΔN) and others.

The HOMO energy is associated with the electron donating ability of a molecule. High value of HOMO energy affirm that the molecule is prone to donate electrons to appropriate acceptor molecule with low energy and empty molecular orbital, hence show better inhibition efficiency. On the contrary, LUMO energy indicates the ability of the molecule to accept an electron. It is worth notice that the molecules that lower LUMO energy value have more electron accepting ability. Therefore, the reactive ability of inhibitor molecule is considered to be closely related to their frontier molecular orbitals, the HOMO and LUMO (Madkour and Elshamy, 2016; Khadom).

According to the value of E_{HOMO} from Table 1, the inhibition efficiency of the molecules follows the sequence: SPE > PPE. On the other hand the inhibition efficiency of the inhibitor molecules in terms of LUMO energy follows the order: PPE > SPE.

The energy gap (ΔE) is an important parameter in describing the adsorption reactivity of inhibitor molecules on metal surface. As ΔE decreases the reactivity of the molecules increases, lower value of energy difference will render good inhibition efficiency because little energy is needed to remove an electron from the highest occupied molecular orbital (Ali-Shattle *et al*. 2021; Lawal and Bashir, 2022). According to the value of ΔE in Table 1 the trend in inhibition efficiency follow: PPE > SPE.

Table 1: Calculated quantum chemical parameters of the studied inhibitor molecules

Parameters	Inhibitors	
	SPE	PPE
HOMO (Orbital number)	77	84
LUMO (Orbital number)	78	85
E_{HOMO}	-7.048	-8.138
E_{LUMO}	0.040	-1.326
Energy gap (ΔE) (eV)	7.088	6.812
Molecular weight (gmol^{-1})	278.14	318.14
Ionization potential (I) (eV)	7.048	8.138
Electron Affinity (A) (eV)	-0.040	1.326
Global hardness (η)	3.5440	3.4060
Global softness (σ)	0.2822	0.2936
Absolute Electronegativity (χ)	3.5040	4.7320
Fraction of Electron Transfer (ΔN)	0.7885	-0.7527
Energy of back-donation (ΔE_{b-d})	-0.8860	-0.8515
Nucleophilicity (ε)	0.5773	0.3042
Electrophilicity (ω)	1.7322	3.2871

$\chi_{Fe} = 4.026 \ eV \quad \eta_{Fe} = 3.875 \ eV$

HSAB (Hard-Soft-Acid-Base) principle introduced by Pearson has been used to describe the binding predilection of inhibitor molecules towards metal surface. The principle states that "hard acids prefer to coordinate to hard base and soft acids prefer to coordinate to soft base" (Madkour and Elshamy, 2016). The principle also points out that bulk metals are chemically the softest materials, as such soft inhibitors give stronger bond with better inhibition efficiency (Umaru and Ayuba, 2020a).

Contrarily, chemical hardness is the resistance against electron cloud polarization or deformation of chemical species. From the definition one can understood, chemical hardness of a molecules and its inhibition efficiency are inversely proportional to each other because hard molecule are disinclined to give electrons. Chemical hardness, softness and ΔE are quantum chemical parameters that are closely related to each other (Kaya *et al*. 2016; El Ibrahimi *et al*. 2018). It is well known that both hardness and softness were derived from the value of HOMO and LUMO orbital energies as a result of Koopman's theorem.

Hard molecules with high HOMO-LUMO energy gap cannot act as good corrosion inhibitor. However, soft molecules with low HOMO-LUMO energy gap are good corrosion inhibitors because they can easily give electron to metals. Normally, inhibitor with the least value of global hardness (hence the highest value of global softness) is expected to have the highest inhibition efficiency (Ali-Shattle *et al*. 2021). From the result given in Table 1 the molecule can be rank in terms of their inhibition efficiency with regard to hardness and softness as follows: PPE > SPE.

The fraction of electron transferred from molecule to the metal surface (ΔN) was calculated accorfing to the Pearson method and was presented in Table 1. It has been proposed by Guo *et al*. (2020); Lawal and Bashir (2022) that if $\Delta N > 0$, the corrosion inhibitor transfers its electrons to metal and vice versa if $\Delta N < 0$. The positive value of ΔN for SPE from Table 1 shows that the inhibitor molecule has a high tendency to donate electron to the empty orbital of metal as contrary to PPE molecule that have negative value of ΔN. Ionization potential (I) and electron affinity (A) of the molecule were calculated from application of Koopman's theorem as expressed in equation (3 & 4), and their values were used in calculating other parameters such as electronegativity and global hardness.

The activity of SPE and PPE as corrosion inhibitors for mild steel has been further analyzed by evaluating the energy of back donation (ΔE_{b-d}), electrophilicity index (ω) and nucleophilicity (ε). ΔE_{b-d} is the amount of energy change when an inhibitor molecule receives and back-donates certain amount of charge. This parameter is explain based on the report (Umaru and Ayuba, 2020a; Udhayakala *et al*. 2012), according to their report when a molecule receives and back-donate equal amount of charge, the total energy change or energy of back-donation (ΔE_{b-d}) is the sum of energy received and back donated. Thus, the most favorable situation corresponds to the case when the total energy change (ΔE_{b-d}) is minimum. Therefore, the value of (ΔE_{b-d}) for both inhibitor molecules are presented on Table 1, and their values are less than zero which indicate that the charged transfer to inhibitor molecules and back-donate is energetically favoured.

The electrophilicity index (ω) is the ability of the molecule to attract electrons while nucleophilicity (ε) is the tendency to donate or shared electrons with others. thus the larger the electrophilicity index value of an inhibitor molecule (a good electrophile), the less effective the molecule will be in inhibiting corrosion, whereas for nucleophilicity, the effectiveness increases with increasing nucleophilicity value (Udowo, 2018; Madkour and ElShamy, 2016). In light of this the activity of the inhibitor molecule base on the value of electrophilicity index and nucleophilicity in Table 1 are in order of : SPE > PPE.

Local Reactivity and Fukui Indices

For the sake of ascertain the reactive center in the molecule with respect to electrophilic and nucleophilic attack, local reactivity of each molecule was evaluated by means of Fukui indices. F^+ measures reactivity with respect to nucleophilic attack or ability to release an electron, while F^- measures reactivity with respect to electrophilic attack or the tendency to accept an electrons. High values of f^+ mark the points of nucleophilic attack, while high value of f^- indicate the points of electrophilic attacks in the molecule (Ayuba and Umar, 2021). The calculated Fukui indices for individual atom of each molecule are presented in Table 2, nonetheless, the active site that is responsible for nucleophilic and electrophilic attack is positioned on atom possessing the highest absolute value of F^+ and F^- respectively.

It can be observed from the result in Table 2, that for SPE, with regard to both Mulliken and Hirshfeld, the active site for nucleophilic attack is located on S(1) of the sulfurous acid which has the highest absolute value (0.509 for Mulliken and 0.345 for Hirshfeld) where as, the electrophilic attack is positioned on O(2) of the carbonyl of ester which contain the highest absolute value (0.293 for Mulliken and 0.233 for Hirshfeld).

With regard to PPE, the nucleophilic centre is located at O(4) of the ester linkage with the highest absolute value (0.278 for Mulliken and 0.246 for Hirshfeld) while the electrophilic centre is located C(2) of the fluoro carbon with 0.069 for Mulliken and C(17) of the alkyl carbon with 0.055 for Hirshfeld. It is imperative to note that for SPE the most susceptible site for nucleophilic and electrophilic attack are on S(1) and O(2) while for PPE is O(4) and C(2) attached to heteroatoms. These could be due to the fact that heteroatoms plays a vital role in deciding the center of nucleophilic and electrophilic attacks on the studied molecule with respect to their potentials as corrosion inhibitors (Ayuba *et al*. 2020). Subsequently, it gives strong adsorption energy and leads to better inhibition efficiency.

The second order Fukui functions (f^2) values of the two inhibitor molecules are presented on Figure 4 & 5, and the percentage value for nucleophilic and electrophilic attack are presented in Table 3. It is observe from both the Figures and the Table that the two inhibitor molecules prefer electrophilic attack than nucleophilic attack, these may be refer to the ability of the molecules to accept an electron through back donation to coordinate with metal surface and thus make act as good inhibitor.

According to Umaru and Ayuba, (2020a) an atom will prefer nucleophilic attack if $f^2 > 0$, and electrophilic attack if $f^2 < 0$. The chart provide the percentage f^2 in positive value with respect to nucleophilic while the negative values in favor of electrophilic attack, and the Table 3 provide the calculated percentage with respect to both nucleophilic and electrophilic attack.

Table 2: Calculated Fukui Indices for the Studied Inhibitor Molecules

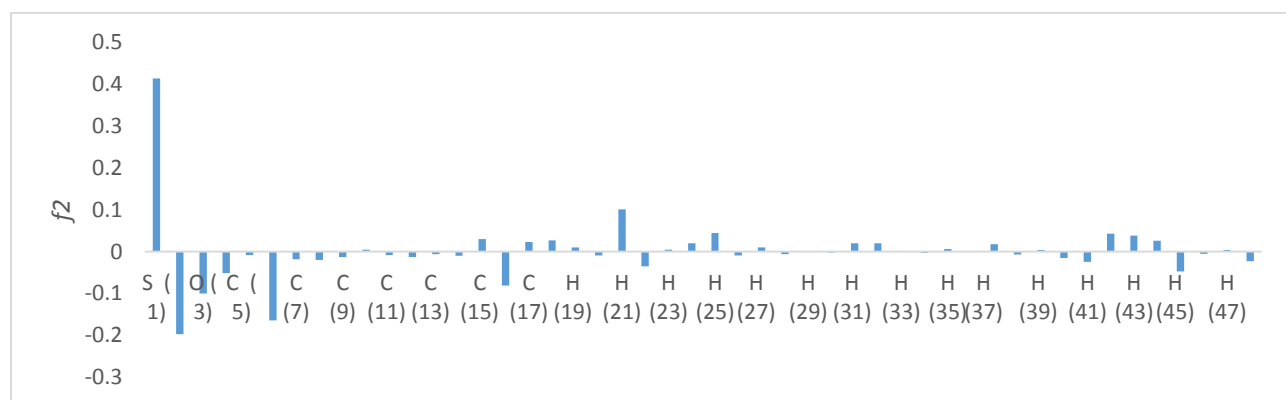| | Nucleophilic (F^+) | | | | Electrophilic (F^-) | | | |
| | Mulliken | | Hirshfeld | | Mulliken | | Hirshfeld | |
Molecule	Atom	Value	Atom	Value	Atom	Value	Atom	Value
SPE	S(1)	0.509	S(1)	0.345	O(2)	0.293	O(2)	0.233
PPE	O(4)	0.278	O(4)	0.246	C(2)	0.069	C(17)	0.055

Figure 4: f^2 values with respect to nucleophilic and electrophilic attack in SPE
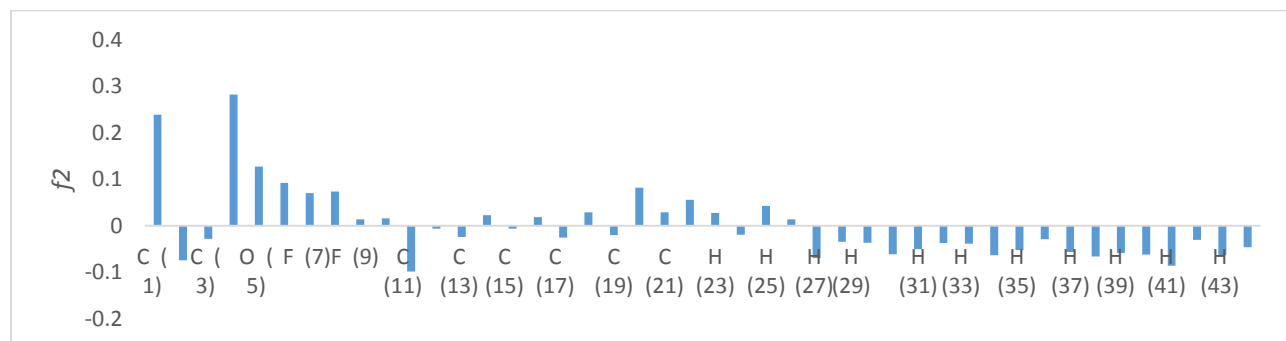

Figure 5: f^2 values with respect to nucleophilic and electrophilic attack in PPE

Table 3: Percentage value for nucleophilic and electrophilic attack for Inhibitor Molecules

| Molecules | SPE | | PPE | |
	Nucleophilic (f^{2+})	Electrophilic (f^{2-})	Nucleophilic (f^{2+})	Electrophilic (f^{2-})
	35.41 %	52.08 %	38.63 %	61.36 %

Molecular dynamic simulation

Molecular dynamic simulation provide in-depth knowledge about the interaction between the inhibitor molecules and metal surface. Such insight knowledge can be understood from discussing the extent of adsorption of inhibitor molecule on metal surface based on the kind of interaction and binding energy (Obi-Egbedi and Ojo, 2015; Lawal and Bashir, 2022). Molecular dynamic simulation was carried out using forcite quench dynamic in order to examine the adsorption behavior of the studied inhibitor molecules on Fe (1 1 0) surface and analyze their interaction. Geometry optimized structure of the molecules were used for the simulation, the atomic coordinates were adjusted based on COMPASS II forcefield until and unless the total energy reach minimum value. The equilibrium adsorption configuration of the two studied molecules are presented in Figure 4 & 5(a & b), it can be observed from the Figures that both molecules are adsorbed on Fe (1 1 0) surface in parallel orientation through sulfur and oxygen atoms as well as other heteroatoms.
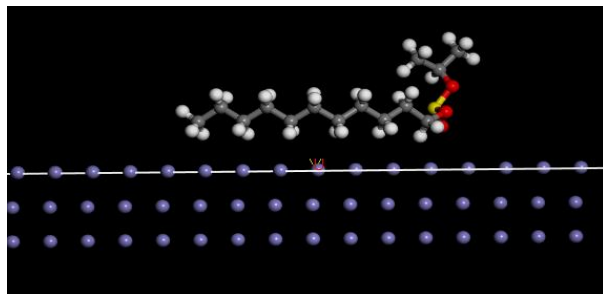

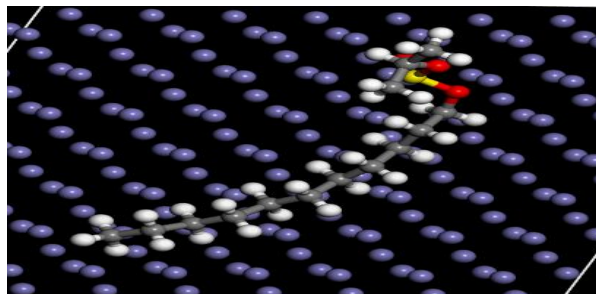Figure 4a: Equilibrium adsorption configuration

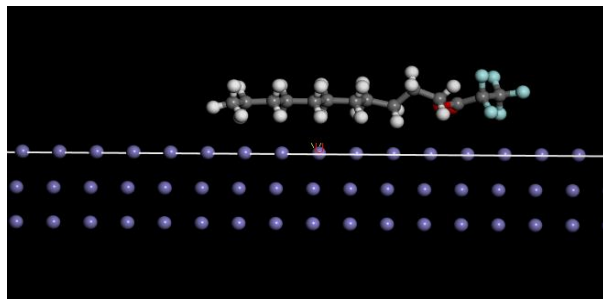 of SPE side view

Figure 4b: Top view of SPE

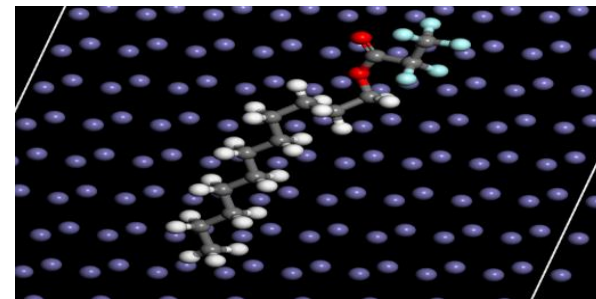Figure 5a: Equilibrium adsorption configuration

of PPE

Figure 5b: Top view of PPE

In addition, Table 4 shows the adsorption and binding energies of the studied inhibitors on the Fe (1 1 0) surface. It is imperative to note that high binding or adsorption energy leads to more stable inhibitor/surface interaction and thus provide higher inhibition performance (Kaya *et al*. 2016). The negative value suggests that spontaneous adsorption may be expected (Guo *et al*. 2020). The order of inhibition efficiency of the studied molecules in terms of their adsorption energy follows the trend SPE > PPE.

The difference in their inhibition efficiency may be attributed to some factors which comprise but not limited to; number of available adsorption sites on the molecules, ionization potential, nature of heteroatom,

charge densities, polarity, molecular size, mode of interaction of the molecules with Fe surface, formation of metallic complexes among others (Ayuba *et al*. 2020).

Table 4: Calculated molecular dynamic simulation parameters for the studied molecules

Properties (kcal.mol^{-1})	Molecules	
	SPE	PPE
Total Kinetic Energy	39.06 ± 9.65	28.30 ± 2.64
Total Potential Energy	-178.85 ± 14.3	-136.39 ± 0.11
Energy of Molecule	-49.79 ± 11.8	-21.35 ± 1.02
Energy of Fe (1 1 0) Surface	0.00 ± 0.00	0.00 ± 0.00
Binding Energy	-129.06	-115.04
Adsorption Energy	129.06 ± 25.8	115.04 ± 1.09

It was reported in literature that adsorption energies greater than 100Kcal/mol or binding energy greater than -100Kcal/mol are associated with chemical adsorption, while values lower than that signifies physical adsorption (Ayuba *et al*. 2018b). Consequently, all the molecules could be said to adsorb chemically on Fe(1 1 0) surface with SPE having higher binding energy. Therefore, SPE inhibitor molecule is said to have provided better protection on mild steel surface than PPE.

CONCLUSION

Theoretical studies was employed using density functional theory (DFT) and molecular dynamic simulation in order to investigate the structural, electronic and reactivity parameters in relation to adsorption of studied inhibitor molecules on mild steel surface, and the following are the outline conclusion:

i. The reactivity centers for SPE are both heteroatoms unlike PPE, these facilitate SPE to have better inhibition efficiency. This show that adsorption of these molecules on mild steel surface involves transfer of lone pair of electron (chemisorption).
ii. The molecules are adsorbed through sulfur and oxygen atom adjacent to the ester functional group as can be observed from the snapshot view of the equilibrium adsorption configurations.
iii. The adsorption energy of the molecule onto the mild steel surface are in order: SPE > PPE.

These shows that SPE have better adsorption energy/binding energy than PPE, which makes it to have better inhibition efficiency on mild steel surface. Also, both DFT and molecular dynamic simulation result are in good agreement with each other, as such theoretical studies can be implemented to design promising corrosion inhibitors without performing any experiment in the lab, and then utilized it for experimental purposes.

REFERENCES

Abakedi O. U. and Asuquo J. E., (2016). "Corrosion Inhibition of Aluminium in Acidic Medium by Ethanol Leaf Extract of *Azadirachta indica"*. *J. basic appl. Res.* 2(4): 556-560.

Ajanaku K. O., Aladesuyi O., Ajanaku C. O., Adedapo E. A., Akinsiku A. A., and Sodiya F. E., (2015). "Adsorption properties of *Azadirachta indicia* extract on corrosion of Aluminium in 1.85 M Hydrochloric acid". *J. Advance Research in Applied Science*, 2(2): 43-52.

Ali-Shattle, E. E., Erteeb, M. A., Khalil, S. M., Berbash, H. A., and Elshawi, Z. E., (2021). Computational Studies (DFT) and PM3 Theories on Thiophene Oligomers as Corrosion Inhibitors for Iron. *American Journal of Chemistry*, 11(1): 1-7.

Al-Mazaideh, G. M., Al-Zereini, W. A., Al-Mustapha, A. H., and Khalil, S. M., (2016). The effect of nitro maleimides from a marine vibrio species compounds as a new source of environmentally friendly corrosion inhibitors for metals. *Advances in Environmental Biology*, 10(8): 159-168.

Ayuba, A. M., and Umar, U., (2021). Modeling Vitexin and Isovitexin Flavones as Corrosion Inhibitors for Aluminium Metal. *Karbala International Journal of Modern Science,* 7(3): 1-12.

Ayuba, A. M., Thomas, A. N., and Abdulfatah, S. M., (2020). Density functional theory and molecular dynamic simulation studies on the corrosion inhibition of some thiosemicarbazide derivatives on aluminium metal. *Journal of Applied Surfaces and Interfaces*, 8: 7-14.

Ayuba, A. M., Uzairu, A., Abba, H., and Shallangwa, G. A., (2018a). Theoretical study of aspartic and glutamic acids as corrosion inhibitors on aluminium metal surface. *Mor. J. Chem.*, 6(1): 160-172.

Ayuba, A. M., Uzairu, A., Abba, H., Shallangwa, G. A., (2018b). Hydroxycarboxylic acids as corrosion inhibitors on aluminium metal: Computational Study. *Journal of Materials and Environmental Sciences*, 9(11): 3026-3034.

Benedetti, A. V., Teixeira, D. A., Valente Jr, M. A. G., Feliciano, G. T., da Silva, S. C., and Fugivara, C. S., (2015). Experimental and Theoretical Studies of Volatile Corrosion Inhibitors Adsorption on Zinc Electrode. *J. Braz. Chem. Soc.,* 26(3): 434-450.

Dubey, R. S., (2020). "Green Corrosion Inhibitos for Metals and Alloys: A Comprehensive Review". *International Journal of Advance Research*. 8(6): 1558-1565.

El Ibrahimi, B., Jmiai, A., El Mouaden, K., Oukhrib, R., Soumoue, A., El Issami, S., and Bazzi, L., (2018). Theoretical evaluation of some α-amino acids for corrosion inhibition of copper in acidic medium: DFT calculations, Monte Carlo simulations and QSPR studies. *Journal of King Saud University-Science*. https://doi.org/10.1016/j.jksus.2018.04.004

El-Hendawy, M. M., Kamel, A. M., Mohamed, M. M. A., Boukherroub, R., Ryl, J., and Amin, M. A., (2021). Diaryl sulphide derivatives as potential iron corrosion inhibitors: A Computational Study. *Molecules*, 26: 6312. https://doi.org/10.3390/molecules26206312.

Elmsellem, H.,Lahmidi, S., Sebbar, N. K., El Ouasif, L., Jilalat, A. E., Elyoussfi, A., Dafali, A., Hammouti, B., El Mahi, B., Essassi, E. M., and Abdel-Rahman, I., (2017). "Corrosion inhibition of mild steel by two new 1,2,4-triazolo[1,5-a] pyrimidine derivatives in 1 M HCl: Experimental and computational study". *Journal of materials and Environmental Sciences*. 8(1): 225-237.

Guo, L., Tan, J., Wu, D., Wang, S., Yu, R., Zhang, F., and Kaya, S., (2020). Electrochemical and Computational Studies on the Corrosion Inhibition of Mild Steel by 1-Hexadecyl-3-methylimidazolium Bromide in HCl medium. *Int. J. Electrochem. Sci.*, 15: 1893-1903.

Jane, N. M., and Nakara, M. T., (2019). "Determination of the Corrosion Inhibition Effect of *Terminalia Ivorensis* Leave Extract on Galvanized and Mild Steel in Sulphuric Acid Media". *American Journal of Physical Chemistry*. 8(1): 11-16.

Kaya, S., Guo, L., Kaya, C., Tuzun, B., Obot, I. B., Touir, R., and Islam, N., (2016). Quantum chemical and molecular dynamic simulation studies for the prediction of inhibition efficiencies of some piperidine derivatives on the corrosion of iron. *Journal of the Taiwan Istitute of Chemical Engineers*, 000: 1-8.

Khadom, A. A., (2017). Quantum Chemical Calculations of Some Amines Corrosions Inhibitors/Copper Alloy Interaction in Hydrochloric Acid. *J. Mater. Environ. Sci.*, 8: 1153-1160.

Khaled, K. F., and Muhammad, A. A., (2009). Electrochemical and Molecular Dynamic Simulation Studies on the Corrosion Inhibition of Aluminium in Molar Hydrochloric Acid using Imidazole Derivatives. *J. Appl. Electrochem.,* 939:2553-2568.

Lawal, S. M., and Bashir, M. I., (2022). Corrosion Inhibition of Zinc in 0.5 M HNO_3 using *Azadirachta Indica* Extract: Experimental and Computational Study. *Bayero Journal of Pure and Applied Sciences*, 13(1): 1.

Madkour, L. H., and Elshamy, I. H., (2016). Experimental and Computation Studies on the Inhibition performances of benzimidazole and it's derivatives for the corrosion of copper in nitric acid. *Int. J. Ind. Chem.*, **7:** 195-221.

Obi-Egbedi, N. O., and Ojo, N. D., (2015). Computational studies of the corrosion inhibition potentials of some derivatives of 1H-Imidazo [4, 5-F] [1, 10] phenanthroline. *Journal of Science Research*, 14: 50-56.

Oke, G. O., Aluko, A. O., and Sanya, O. T., (2018). "Inhibitive potential of *Datura strmonium* leaf extract on the corrosion behavior of mild steel in 1M HCl acidic solution". *Leonardo Journal of Sciences*, (32): 76-92.

Sahin, M., Gece, G., Karci, F., and Bilgic, S., (2008). Experimental and Theoretical Study of the Effect of Some Heterocyclic Compounds on the Corrosion of Low Carbon Steel in 35% NaCl Medium. *J. Appl. Electrochem.*, 38: 809-815.

Sharma S. K., Peter A., and Obot I. B., (2015). "Potential of *Azadirachta indica* as a green corrosion inhibitor against mild steel, aluminum, and tin: a review". *Journal of Analytical Science and Technology*, 6(26): DOI 10.1186/s40543-015-0067-0.

Srikanth, A. P., and Sivakumar, P. R., (2020). "Green corrosion inhibitor: A comparative study". *Sadhana indian Academy of Science*. https://doi.org/10.1007/s12046-020-1283-x

Udhayakala, P., Rajendiran, T. V., and Gunasekaran, S., (2012). Density Functional Theory Investigations for the adsorption of some Oxadiazole Derivatives on Mild Steel. *Journal of Advanced Scientific Research*, 3(3): 67-74.

Udowo, V. M., (2018). Computational Studies of the Corrosion Inhibition Potential of Quercetin and Coumarin. *Archives of Organic and Inorganic Chemical Sciences*, Lupine Publishers, ISSN: 2637-4609. **DOI:** 10.32474/AOICS.2018.02.000133

Umaru, M and Ayuba, A. M., (2020a). Computational studies of Anticorrosive Effect of Some Thiazole Derivatives Against the Corrosion of Aluminium. *RHAZES Academic Scienctific Journals*, 10: 113-128.

Umaru, M., and Ayuba, A. M., (2020b). Quantum chemical calculations and molecular dynamic simulation studies on the corrosion inhibition of aluminium metal by myricetin derivatives. *Journal of New Technology and Materials*, 10(02): 18-28.

Zarrouk, A., Zarrok, H., Assouag, M., Oudda, H., Hallaoui, A., Touzani, R., Allali, M., Hammouti, B., El Hezzat, M., and Bouachrine, M. (2015). Quantum Chemical Study on the Corrosion Inhibition of Some Bipyrazoles. *Res. J. Pharm., Bio. and Chem. Sci.*, 6(4): 1853-1860.